PHYSICAL REVIEW B

CONDENSED MATTER AND MATERIALS PHYSICS

THIRD SERIES, VOLUME 60, NUMBER 4 15 JULY 1999-II

RAPID COMMUNICATIONS

Rapid Communications are intended for the accelerated publication of important new results and are therefore given priority treatment both in the editorial office and in production. A Rapid Communication in **Physical Review B** *may be no longer than four printed pages and must be accompanied by an abstract. Page proofs are sent to authors.*

Dynamical electron-ion coupling in the ionic conductor α-NaSn

Masayasu Miyata, Takeo Fujiwara, Susumu Yamamoto, and Takeo Hoshi
Department of Applied Physics, University of Tokyo, Bunkyo-ku, Tokyo 113-8656, Japan
(Received 12 May 1999)

Dynamical electron-ion coupling in an ionic solid NaSn at high temperatures is studied by *ab initio* molecular dynamics simulation. The cooperative ion dynamics of the migration of Na^+ ions and the deformations of $(Sn_4)^{4-}$ tetrahedra are clarified. The band gap fluctuates between metallic and semiconducting values, and is strongly coupled with the ion dynamics. When the band gap vanishes, the character of the highest occupied eigenfunction changes from bonding to nonbonding within a tetrahedron, and it is caused by the deformations of the tetrahedra. The mechanism of the rapid rise of conductivity experimentally observed is discussed in light of our results. [S0163-1829(99)50132-X]

The high temperature solid phase of NaSn, α-NaSn between 757 and 854 K, shows anomalous behavior of conductivity which rises rapidly with temperature from semiconducting (about $5\ \Omega^{-1}\,cm^{-1}$) to metallic (about $2000\ \Omega^{-1}\,cm^{-1}$) values.[1] The lower temperature solid phase, β-NaSn (0–757 K), is semiconducting, with a band gap $E_g = 0.74$ eV, in which charge transfer and directional bonding lead to the formation of $(Sn_4)^{4-}$ tetrahedral polyanions. The melting point of α-NaSn is 854 K and $(Sn_4)^{4-}$ tetrahedra survive even in the metallic liquid phase.[2] The large enthalpy change of $4.95\ J\,mol^{-1}\,K^{-1}$ at the α-β phase transition indicates that α-NaSn is dynamically disordered. The great attenuation and broadening of Bragg peaks at large wave number (around $2\ Å^{-1}$) obtained by the neutron scattering experiment show diffusive ion dynamics in α-NaSn.[3,4] These experimental facts suggest a strong coupling between diffusive ion motion and conductivity.

In this paper we report the results of *ab initio* molecular dynamics (AIMD) simulation of α-NaSn. By using AIMD, it is shown that the migration of Na^+ ions induces the deformations of $(Sn_4)^{4-}$ tetrahedra, which changes the character of bonding within a tetrahedron. It is also shown that nonbonding states appear due to the bond breaking within a tetrahedron, and the band gap E_g is reduced. As a result, one can expect that the electronic conductivity increases rapidly with temperature, which is consistent with experiments. Metal-insulator crossover of an electron system coupled with ion dynamics provides the possibility of designing materials whose electronic transport is controlled by ion dynamics.

The constant-temperature AIMD simulation has been performed by a direct minimization method[5] of the energy functional of the local density approximation (LDA), and by means of the Nosé-Hoover thermostat technique.[6,7] We used 80 occupied and 14 unoccupied Kohn-Sham (KS) single-electron orbitals $\psi_k(\mathbf{r})$, $(k=1,\cdots,94)$. The Γ point was only used in the Brillouin zone and the KS orbitals were expanded in 6849 plane waves with an energy cutoff $E_{cut} = 10$ Ry. We used the Gaussian form as the entropy term related to the electron occupation f_k.[8] Also, we adopted the normconserving pseudopotential suggested by Hamann *et al.*[9] with the Kleinman-Bylander separable form.[10] The local exchange correlation functional of Ceperly and Alder[11] was used. The equations of motion of ions and the thermostat were solved by using Verlet's algorithm.[12] A tetragonal cell of $a = b = 10.46$ Å, $c = 17.39$ Å was used as a simulation cell under the periodic boundary condition. This cell corresponds to the primitive cell of solid β-NaSn and contains 32 Na atoms and 32 Sn atoms. A volume expansion and symmetry change occur at the α-β transition.[3,13] We neglect these changes because the differences are small.

The initial atomic configuration in this simulation is that of the β-NaSn structure.[14] It has eight $(Sn_4)^{4-}$ tetrahedra, and the edge length of a tetrahedron is 2.97 Å. The mass centers of $(Sn_4)^{4-}$ form a tetragonal lattice structure. Na^+

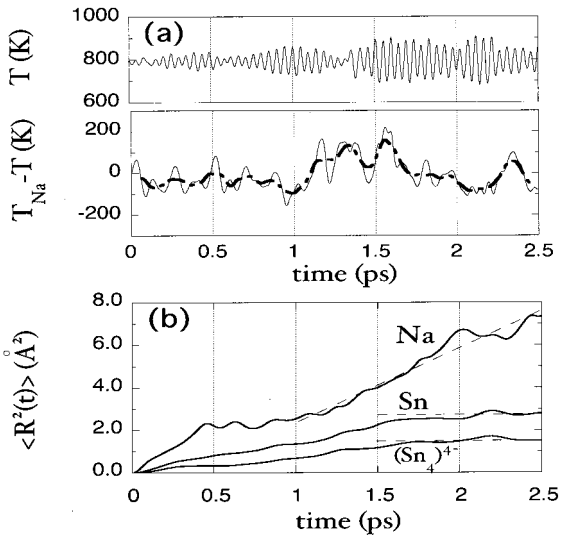

FIG. 1. (a) Instantaneous temperature T, $T_{\mathrm{Na}}-T$ (K). The bold chain line is the average of $T_{\mathrm{Na}}-T$ of which the value at time t is obtained by averaging from $t-0.125$ ps to $t+0.125$ ps. (b) Mean square displacement $\langle R^2(t)\rangle$ (Å^2) for three species. The dashed lines are drawn as guides to the eye to show the tendencies of motions.

ions and $(Sn_4)^{4-}$ tetrahedra are densely packed and the tetrahedra are kept as far apart as possible. The nearest neighbor distances of Na-Na, Na-Sn, and Sn-Sn in the different tetrahedron are 3.62–3.72 Å, 3.35–3.53 Å, 3.76 Å, respectively. The simulation was performed for 3.5 ps. To obtain the results after equilibration, we discarded the produced data of initial 1 ps, and adopted those of sequential 2.5 ps in the present simulation. The temperature was set and controlled at 790 K to reproduce the dynamics of α-NaSn. During the simulation, the constant of the Nosé-Hoover dynamics E_{NH} was kept within $|\Delta E_{\mathrm{NH}}|\leqslant 2.2\times 10^{-5}$ Ry/atom, $|\Delta E_{\mathrm{NH}}/E_{\mathrm{NH}}|\leqslant 5.7\times 10^{-6}$.

Figure 1 shows the time evolution of the physical quantities describing the ion dynamics. The instantaneous temperature T_A for A ($A=$Na,Sn) is defined as $\frac{3}{2}N_A k_{\mathrm{B}}T_A=\Sigma_{n\in A}^{N_A}\frac{1}{2}m_n(\mathbf{V}_n(t))^2$, where m_n and $\mathbf{V}_n(t)$ are the mass and the velocity at time t of the nth atom, N_A is the total number of A atoms, and k_{B} is the Boltzmann's constant. The instantaneous temperature T for the total system is defined as $T=(N_{\mathrm{Na}}T_{\mathrm{Na}}+N_{\mathrm{Sn}}T_{\mathrm{Sn}})/(N_{\mathrm{Na}}+N_{\mathrm{Sn}})$. Figure 1(a) shows the total instantaneous temperature T, and $T_{\mathrm{Na}}-T=-(T_{\mathrm{Sn}}-T)$, where T is subtracted from T_{Na} in order to exclude the short period fluctuation of 50–60 fs, caused by the thermostat dynamics. Temperature control was attained well; the average temperature $\langle T\rangle=792$ K, the fluctuation of temperature $\delta T\equiv(\langle T^2\rangle-\langle T\rangle^2)^{1/2}=44$ K and $\delta T/\langle T\rangle=0.056$. We can find another fluctuation with a longer period in $T_{\mathrm{Na}}-T$ of Fig. 1 (a). The bold chain line is the average of $T_{\mathrm{Na}}-T$ ranging over 0.25 ps at each time t, which clearly shows the fluctuation of longer period; slight increase of $T_{\mathrm{Na}}-T$ at $1<t<1.5$ and $2<t<2.3$, and slight decrease at $1.5<t<2$. The fluctuations of T_{Na} and T_{Sn} are $\delta T_{\mathrm{Na}}=90$ K, $\delta T_{\mathrm{Sn}}=93$ K. Though one considers the difference of number of samples, these fluctuations are much larger than those of T, i.e., $\sqrt{N_{\mathrm{Na,Sn}}}\delta T_{\mathrm{Na,Sn}}>\sqrt{N_{\mathrm{Na}}+N_{\mathrm{Sn}}}\delta T$. This suggests that the kinetic energy transfer between two species occurs periodically, though a certain part of this fluctuation may be due to the smallness of the size of our simulation cell. The kinetic energy flows from Na^+ ions to Sn^- ions for $0.5<t<1$ and $1.5<t<2$ ps, from Sn^- ions to Na^+ ions for $1<t<1.5$ and $2<t<2.3$ ps. Because α-NaSn is an ionic solid, the dynamical coupling between $(Sn_4)^{4-}$ tetrahedra and Na^+ ions is strong.

The mean square displacement (MSD) for A [$A=$Na,Sn,$(Sn_4)^{4-}$] is defined as $\langle R^2(t)\rangle_A=\Sigma_{n\in A}^{N_A}\{\mathbf{R}_n(t)-\mathbf{R}_n(0)\}^2/N_A$. $\mathbf{R}_n(t)$ is the coordinate of the nth atom (cluster) at time t, N_A is the total number of A atoms (clusters). Figure 1(b) shows the MSD for Na, Sn, and the mass center of $(Sn_4)^{4-}$. We observe that the motion of Na^+ ions is diffusive, accompanying two plateaus reflecting the periodic kinetic energy transfer seen in Fig. 1(a). From the Einstein relation, $\langle R^2(t)\rangle=6Dt$, we can evaluate the self-diffusion coefficient of Na^+ ions as $D_{\mathrm{Na}}=5.8\times 10^{-5}$ cm^2/s. This value is comparable with that of the liquid Na at 473 K, 8.1×10^{-5} cm^2/s.[15] Figure 1(b) shows a plateau at $t\simeq 1$ ps which corresponds to the cooling of Na^+ ions as seen in Fig. 1(a). During $1<t<1.5$ ps, the heating of Na^+ ions accelerates the increase of MSD for Na. The cooling of Na^+ ions after $t\simeq 1.5$ ps causes a plateau of MSD for Na again at $t\simeq 2$ ps. The values of MSD for Sn and those of the mass center of $(Sn_4)^{4-}$ increase slowly after $t=1.5$ ps, and are saturated, after $t=2.2$ ps, to the values of 2.7 Å^2 and 1.5 Å^2, respectively. Accordingly, the motions of Sn^- ions and those tetrahedra are not diffusive. The MSD for Sn indicates a large amplitude $\sqrt{\langle R^2(t)\rangle_{\mathrm{Sn}}}=1.6$ Å of fluctuation from the equilibrium lattice point, that is, 53% of the edge length of a tetrahedron. The large amplitude of motions of Sn^- ions is consistent with the large attenuation of Bragg peaks.[3] Again we should point out some possibility that the present system is not equilibrated enough for the relatively small cell size. Independent of the MSD results, we observed that the larger diffusion of Na^+ ions locally induces the larger deformations of $(Sn_4)^{4-}$ tetrahedra. The tetragonal lattice structure of mass centers of $(Sn_4)^{4-}$ had been conserved. Possible motions of Sn^- ions are the rotational motions and/or the internal deformations of $(Sn_4)^{4-}$ tetrahedra.

Because the edge lengths of a tetrahedron obtained here vary between 2.6 and 4.5 Å, the deformations of the tetrahedra must be large. To analyze such deformations of $(Sn_4)^{4-}$ tetrahedra, we calculated the third-order invariant,[16] which is defined as

$$\hat{W}_4^i=\sum_{m_1+m_2+m_3=0}\begin{pmatrix}4 & 4 & 4\\ m_1 & m_2 & m_3\end{pmatrix}Q_{4m_1}^iQ_{4m_2}^iQ_{4m_3}^i\Big/\sum_{m=-4}^{4}|Q_{4m}^i|^3. \tag{1}$$

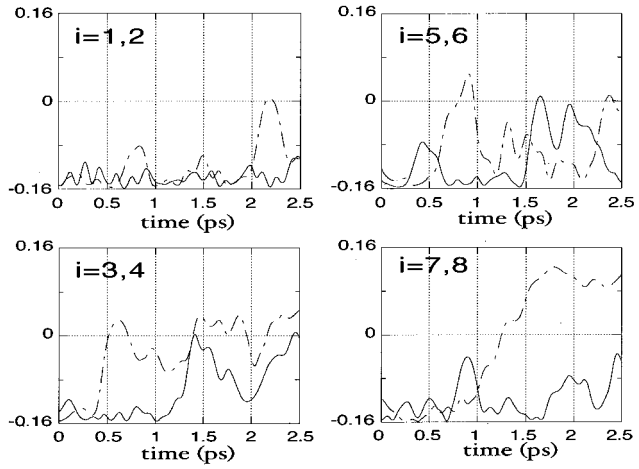

FIG. 2. Time evolution of the third-order invariant $\hat{W}_4^i$ for $i=1,3,5,7$ (chain lines), and for $i=2,4,6,8$ (solid lines).

Here

$$\begin{pmatrix} 4 & 4 & 4 \\ m_1 & m_2 & m_3 \end{pmatrix}$$

is Wigner's $3j$ symbol, $Q_{4m}^i=\Sigma_{k=1}^4 Y_{4m}(\mathbf{r}_k^i)/4$, Y_{lm} is a spherical harmonics, $\mathbf{r}_k^i$ is kth vertex coordinate of ith tetrahedron ($i=1,\ldots,8$) relative to its mass center coordinate; $\hat{W}_4^i=-\frac{7}{3}\sqrt{\frac{2}{429}}\simeq-0.16$ for an ideal tetrahedron. The value of $\hat{W}_4^i$ is sensitive to the deformation of a tetrahedron; for example, the increase of the length of an edge of a tetrahedron by 30% gives $\hat{W}_4^i\simeq 0$. Figure 2 shows the time evolution of $\hat{W}_4^i$. We found that the deformations of tetrahedra are large and their time evolution is synchronous; that is, the recovering of symmetry toward $t\simeq 1$ and 2 ps, and the onset of deformations after that. The tetrahedra of $i=1,3,5,8$ recover those symmetry toward $t\simeq 1$ ps, then those of $i=3,4,7$ starts to deform again. The same process occurs sequentially, as the symmetry recovering of the tetrahedra of $i=3$, 4, 5 toward $t\simeq 2$ ps, and the onset of the deformations of those of $i=1,3,4,5$. The synchronous recovering corresponds to the cooling of Na^+ ions, and the synchronous deformation corresponds to the heating of Na^+ ions, as seen in Fig. 1(a).

We can depict the ion motions as follows. As the result of the strong coupling between two atomic species, a local energy transfer between them occurs periodically. Here, it

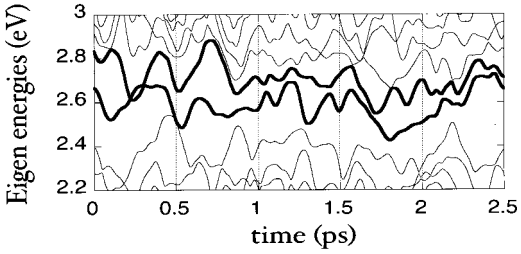

FIG. 3. Time evolution of the eigenenergies near the chemical potential. The energies of the highest occupied and the lowest unoccupied levels are drawn by bold lines.

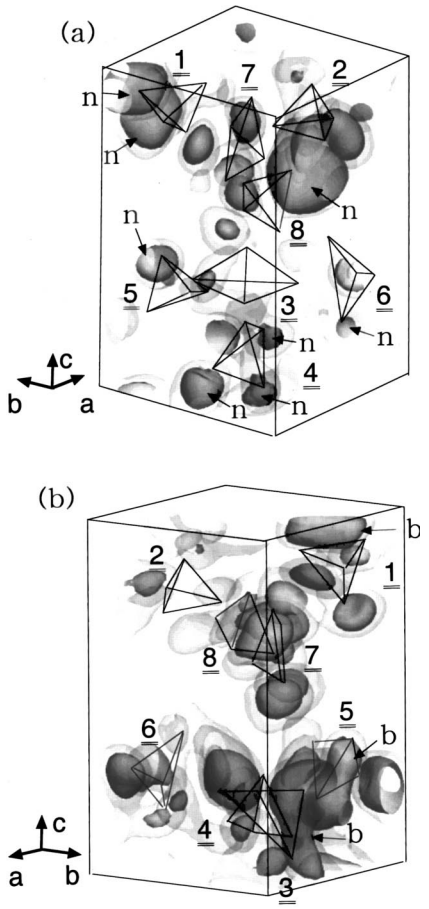

FIG. 4. The snapshots of the $(Sn_4)^{4-}$ tetrahedra and the density distribution of kth KS orbital $|\psi_k(\mathbf{r})|^2$ for (a) $k=80$ with occupancy $f_{80}=0.56$ at $t=1.7$ ps, the case of $E_g=0.03$ eV, and for (b) $k=78$ with occupancy $f_{78}=1.00$ at $t=2.0$ ps, the case of $E_g=0.2$ eV. The densities are represented by isosurfaces at $|\psi_k(\mathbf{r})|^2=3.0/V$ (dense), $1.0/V$ (transparent), where V is the volume of the simulation cell. Each figure is rotated to clearly show the characteristic regions of bonding and nonbonding, which are indicated as *b* and *n*, respectively.

should be stressed that the energy transfer could not be coherent over a macroscopic spatial extent, but only over a microscopic scale of the mean free path. The rise and drop of the kinetic energy of Na^+ ions correspond to the acceleration and deceleration of diffusive motion of Na^+ ions, and to the deformation and recovering of symmetry of $(Sn_4)^{4-}$ tetrahedra.

The eigenenergies of KS orbitals near the chemical potential are shown in Fig. 3, where the energies of the highest occupied and the lowest unoccupied KS orbital are shown in bold lines. Though the level crossings sometimes occur, eigenenergies are separated with an interval of about 0.1 eV, so a band gap E_g can be defined. The wide band gap exists ($E_g\simeq 0.1$–2 eV) for $0.4<t<1$ and $1.7<t<2.1$ ps, while it frequently vanishes for $t\simeq 0.25$ $1<t<1.7$ and $t>2.1$ ps. Thus, E_g fluctuates from semiconducting to metallic values, roughly corresponding to that of the kinetic energy fluctuation between two atomic species. We can expect that the change in E_g is due to a strong coupling between the ion dynamics and electronic states. Again we should stress that the fluctuation of the band gap could not be coherent over a macroscopic spatial extent.

The density of states near the band gap of β-NaSn originates predominantly from bonding and antibonding states within a $(Sn_4)^{4-}$ tetrahedron.[17] The origin of the band gap in α-NaSn is not very different from that of β-NaSn. The chemical potential is positioned in a gap of Sn p states. The occupied p states correspond to a bonding state within a tetrahedron and the empty p states just above the chemical potential correspond to an antibonding state. As a unified understanding of ion dynamics and the electronic states near the chemical potential, we propose the following picture. The diffusive motions of Na^+ ions induce the deformations of $(Sn_4)^{4-}$ tetrahedra. The deformations, namely, the change of the symmetry and the Sn-Sn distances within and between tetrahedra, will change the character of bonding within a tetrahedron into that of nonbonding. Because of the appearance of a nonbonding state, the energy separation between bonding and antibonding states vanishes. The fast migration of Na^+ ions at higher temperatures induces further frequent reduction of the band gap in some local regions of α-NaSn, which causes the enhancement of the bulk electronic conductivity. So we can expect that the temperature dependence of the electronic conductivity of α-NaSn will be stronger than that of activation type.

In order to investigate the character of bonding or nonbonding and its change, we depicted the density distributions of KS orbitals near the chemical potential in several cases. We preliminarily ascertained that a character of bonding within a tetrahedron appears directionally on a side of a tetrahedron by the observation of a highest occupied KS orbital of β-NaSn. Figure 4 shows the density distribution of a KS orbital and $(Sn_4)^{4-}$ tetrahedra of two cases; (a) $\psi_{80}(\mathbf{r})$ with the occupancy of $f_{80}=0.56$, when the band gap nearly vanishes ($E_g=0.03$ eV, $t=1.7$ ps), (b) $\psi_{78}(\mathbf{r})$ with the occupancy of $f_{78}=1.00$, when the wide band gap exists ($E_g=0.2$ eV, $t=2.0$ ps). Comparison between these two cases enables us to investigate not only the character of eigenstates near the chemical potential when the system is metallic or insulating, but also the coupling with the synchronous recovering of symmetry of tetrahedra toward $t\simeq 2$ ps. The character of nonbonding appears in Fig. 4(a), that is, the appearance of the isolated spherical peak on Sn atoms of the tetrahedra of $i=1,4,5,6,8$. On the other hand, the character of bonding appears in Fig. 4(b) on the side of the tetrahedra of $i=1,3,5$. Also, when the wide band gap exists ($t=2.0$ ps), the character of bonding within the other tetrahedra appears in the other KS orbitals near the band gap such as $\psi_{77}(\mathbf{r})$, $\psi_{79}(\mathbf{r})$, and $\psi_{80}(\mathbf{r})$. Though the ionic configurations do not change so much during $1.7<t<2.0$ ps, the character within a tetrahedron has greatly changed. We can expect that the synchronous recovering of symmetry of tetrahedra strongly affects the electronic state near the chemical potential in α-NaSn.

We summarize the present results and discussions. (1) Ion dynamics of α-NaSn is the diffusive motion of Na^+ ions and large deformations of $(Sn_4)^{4-}$ tetrahedra. The mass centers of $(Sn_4)^{4-}$ still keep tetragonal lattice structure. (2) Dynamical coupling of the band gap and ion dynamics determines the characteristic electronic structure of α-NaSn. The fluctuation of the band gap between semiconducting and metallic values, which is neither similar to that for the semiconducting β-NaSn nor to that for the metallic liquid phase, will cause the anomalous temperature dependence of bulk electronic conductivity of α-NaSn. Further conclusive studies might be desired in a larger system in a longer time run in the future.

We thank Y. Ishii for a fruitful discussion when developing the calculation code. The numerical simulations were carried out by the computer facilities at the Institute of Molecular Science at Okazaki, at the Super Computer Center, Kyu-shu University, and at the Institute for Solid State Physics, the University of Tokyo. We also acknowledge the Center for Promotion of Computational Science and Engineering (CCSE) of Japan Atomic Energy Research Institute (JAERI) for the use of the computer facilities. This work was partially supported by a Grant-in-Aid for COE Research and also a Grant-in-Aid from the Japan Ministry of Education, Science, Sport, and Culture.

[1] J. Fortner, M.-L. Saboungi, and J. E. Enderby, Phys. Rev. Lett. **74**, 1415 (1995).
[2] B. P. Alblas, W. van der Lugt, W. Geertsma, and C. van Dijk, J. Phys. F **13**, 2465 (1983).
[3] M.-L. Saboungi, J. Fortner, W. S. Howells, and D. L. Price, Nature (London) **365**, 237 (1993).
[4] D. L. Price, M.-L. Saboungi, and W. S. Howells, Phys. Rev. B **51**, 14 923 (1995).
[5] M. C. Payne, M. P. Teter, D. C. Allan, T. A. Arias, and J. D. Joannopoulos, Rev. Mod. Phys. **64**, 1045 (1992).
[6] S. Nosé, Mol. Phys. **52**, 255 (1984).
[7] W. G. Hoover, Phys. Rev. A **31**, 1695 (1985).
[8] G. Kresse and J. Furthmüller, Comput. Mater. Sci. **6**, 15 (1996).
[9] D. R. Hamann, M. Schlüter, and C. Chiang, Phys. Rev. Lett. **43**, 1494 (1979).
[10] L. Kleinman and D. M. Bylander, Phys. Rev. Lett. **48**, 1425 (1982).
[11] We used the parametrization by Perdew and Zunger; J. P. Perdew and A. Zunger, Phys. Rev. B **23**, 5048 (1981).
[12] L. Verlet, Phys. Rev. **159**, 98 (1967).
[13] J. W. Richardson, D. L. Price, and M.-L. Saboungi, Phys. Rev. Lett. **76**, 1852 (1996).
[14] W. Müller and K. Volk, Z. Naturforsch. B **32**, 709 (1977).
[15] M. Shimoji, *Liquid Metals: An Introduction to the Physics and Chemistry of Metals in the Liquid State* (Academic Press, London, 1977), p. 192.
[16] P. J. Steinhardt, D. R. Nelson, and M. Ronchetti, Phys. Rev. Lett. **47**, 1297 (1981).
[17] E. Springelkamp, R. A. de Groot, W. Geertsma, W. van der Lugt, and F. M. Mueller, Phys. Rev. B **32**, 2319 (1985).